Composites: Part A 175 (2023) 107781

Contents lists available at ScienceDirect

Composites Part A

journal homepage: www.elsevier.com/locate/compositesa

Transparent shape memory polyimide enables OLED for smart deformation

Xinzuo Huang [a,1], Rongxiang Hu [a,1], Fenghua Zhang [a], Yanju Liu [b], Jinsong Leng [a,*]

[a] Centre for Composite Materials and Structures, Harbin Institute of Technology (HIT), No.2 Yikuang Street, Harbin 150000, People's Republic of China
[b] Department of Astronautic Science and Mechanics, Harbin Institute of Technology (HIT), No. 92 West Dazhi Street, Harbin 150000, People's Republic of China

ARTICLE INFO

Keywords:
A. Graphene
A. Smart materials
E. Chemical vapour deposition (CVD)
E. Resin flow

ABSTRACT

An innovative process for producing flexible transparent graphene electrodes has been proposed. The electrochemically polished copper-foil was used as the metal substrate to prepare high-quality monolayer graphene. Monolayer graphene was transferred from copper-foil to transparent shape memory polyimide (TSMPI) intactly by novel flow-casting transfer technology, and the smart, ultra-clean and smooth flexible graphene electrode (pG@TSMPI) was fabricated. The light transmittance of pG@TSMPI at 550 nm is 86%, the average sheet resistance is 310 Ω/sq, and the surface roughness (Ra) is 18 nm. Smart white OLED was manufactured using pG@TSMPI as transparent anode, and its luminescence performance was comparable to that of ITO-based device. Depending on the shape memory effect of TSMPI substrate, the smart OLED has the superiorities of variable stiffness and reconfigurable shape, which can transform from 2D structure into complex 3D structure.

1. Introduction

Transparent electrodes with high conductivity and transparency are the critical components of modern optoelectronic devices such as solar cells, touch screens and organic light-emitting diodes (OLEDs) [1–4]. Among the commercial transparent conductive oxide materials, indium tin oxide (ITO) with low sheet resistance (less than40 Ω/sq) and high light transmittance (>80%) is the most widely used category. [5–7] However, the flexibility of ITO is terrible, devices equipped with ITO electrodes can hardly work after a certain extent of deformation for the destruction of electrode, and it is not quite suitable for flexible electronic devices [8,9]. As a faveolate lamellate two-dimensional material with unique orientation of atoms, graphene exhibits high electron mobility, high transmittance, outstanding mechanical flexibility, and chemical stability, which can be used as an excellent conductive material as well as a transparent electrode [10–12].

The method of fabricating graphene films has been developed extensively and thoroughly, such as the mechanical exfoliation, epitaxial growth, oxidation–reduction, and so on [13–16]. Among these technologies, chemical vapor deposition (CVD), which can produce large scale and high-quality graphene, was regarded as the most promising method to obtain favorable graphene films for the flexible transparent graphene electrodes [7,17]. The graphene layer was usually grown on a metal matrix such as copper foil or nickel foil. To further apply the graphene film to the electronic devices, a transfer process from development substrates onto targeted substrates was unavoidable. It generally involves two transfer processes from the growth substrates to the target substrates with the help of a transfer medium. With the constant effort of researchers, ingenious methods have been verified as effective ways to transfer graphene, such as wet transfer, dry transfer, roll-to-roll transfer, support-free transfer, and so on [18–21]. Zhang et al. [22] transferred single-layer graphene to glass slides and SiO_2 substrates by the wet transfer method with the assistance of PMMA. It points out that the electrical properties of the produced graphene will be significantly influenced by the PMMA residue. There are still structure defects of delamination and cracking during the wet transfer process. Li et al. [21] reported a roll-to-roll dry transfer process for large-scale graphene grown by CVD. With simultaneous control of peeling tension and speed, the roll-to-roll dry transferred graphene possesses a flatter structure than those fabricated with wet-chemical etched graphene, and the electrical sheet resistance is up to 9.5 kΩ sq $^{-1}$, meanwhile, it also avoids chemical contamination and allows the reuse of graphene growth substrates. Liu et al. [23] carried out a direct and polymer-free transfer process of CVD grown graphene from the Cu substrate to a smooth PET substrate, which pretreated by a facile solution method. The transferred graphene possesses the high transmittance and excellent mechanical stability of the original graphene layer, and the prepared flexible OLED devices exhibit excellent performance. It can be seen that the transfer

* Corresponding author.
E-mail address: lengjs@hit.edu.cn (J. Leng).
[1] These authors contributed equally to this work.

https://doi.org/10.1016/j.compositesa.2023.107781
Received 11 April 2023; Received in revised form 4 September 2023; Accepted 5 September 2023
Available online 9 September 2023
1359-835X/

technology of graphene will affect the performance of devices dramatically, especially in flexible electronic devices. However, the multiple transfer process of graphene film may lead to irreversible damages, such as physical wrinkles, breakage, and chemical contamination, which will cause the delamination of graphene and affect the performance of the corresponding devices [24,25]. In addition, the conventional preparation method of flexible graphene electrodes for OLED requires the substrates to maintain an absolute plane state, and the obtained flexible device was a planar constructure without external support. [26] With the growing demand for complex three-dimensional flexible devices, the graphene electrodes need an extra brace to fix with the cambered substrates.

Shape memory polymers (SMP), as one kind of smart material, possess the property of altering the shape and modulus induced by an external stimulus, which could endow more functions with flexible electronic devices and thus enable some novel applications [27–31]. Some flexible transparent electronic devices have been fabricated by using SMP as substrate or encapsulation layer, such as SMP-based light-emitting diodes and thin film transistors, and the transparent substrate including thiol/acrylate SMP, crosslinked shape memory polyacrylate and shape memory poly(*tert*-butylacrylate) [32–34]. Pei et al. [33] integrated the transparent shape memory polyacrylate and silver nanowires into a flexible electrode, which possesses a low surface resistance, and the prepared light-emitting diode exhibits a sound luminous efficacy. In addition, the device could deform actively at 120 °C with decent shiny brightness. Kippelen et al. [32] reported a green electrophosphorescent OLED based on bio-compatible SMP substrates, which can be used for wearable electronic applications. The SMP based OLEDs exhibit a maximum efficacy of 33 cd/A at a luminance of 1000 cd/cm^2, and the bio-compatible SMP substrates endow OLEDs with the property of intelligent deformation, which bring the devices a new branch of application, such as conformable smart skin devices, minimally invasive biomedical devices, and flexible lighting/display technologies. Different SMP based devices can be used for different applications, however, with

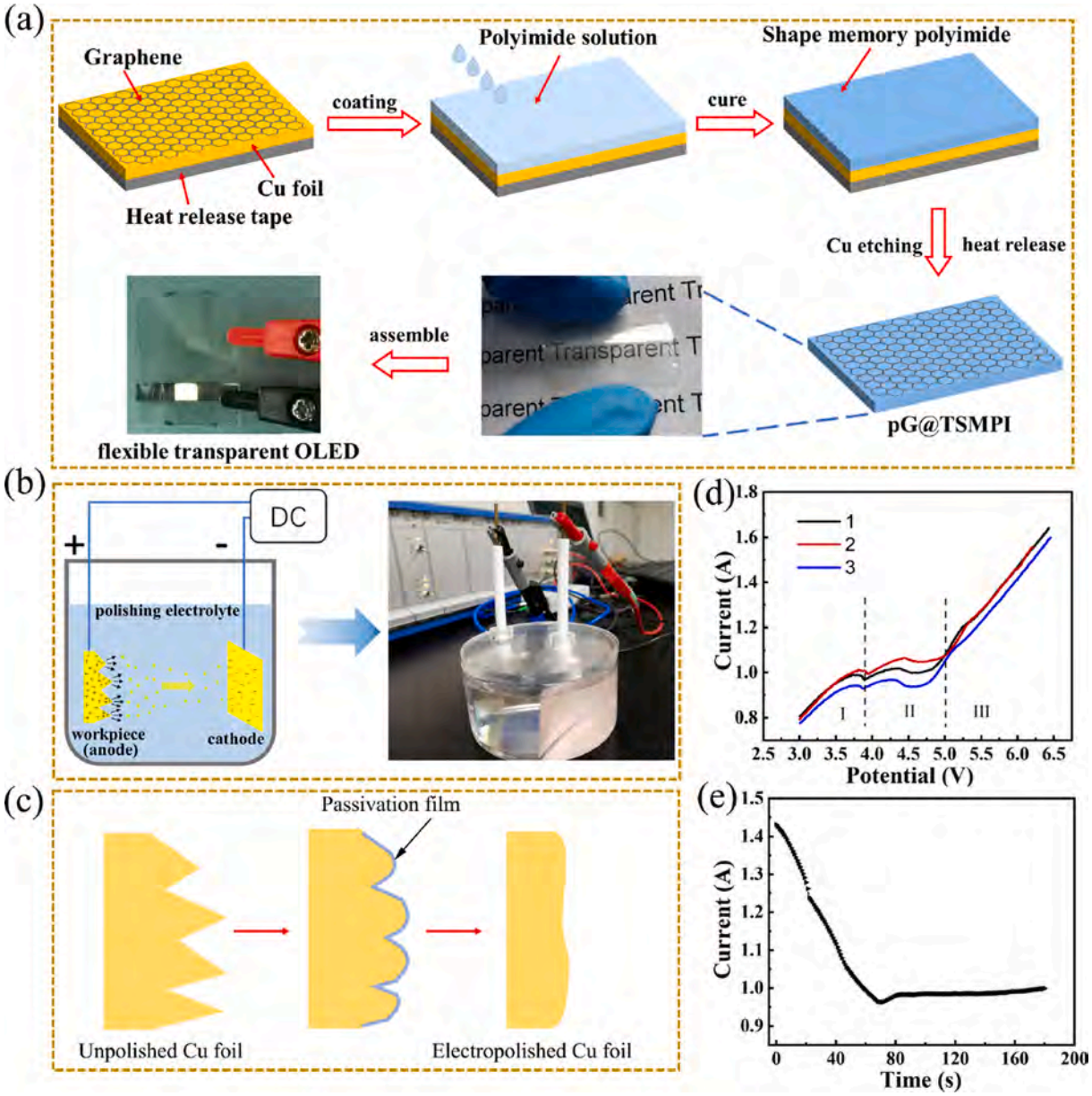

Fig. 1. a) schematic diagram of graphene transfer process by flow-casting method; b) schematic diagram and digital photo of the electrochemical polishing device; c) mechanism of electrochemical polishing of copper foil; d) the volt-ampere characteristic curve of copper foil; e) variation of current with time during electrochemical polishing.

the increasing complexity of the application of flexible electronic devices, the general SMP substrate can hardly meet the demands of special occasions, especially the wide operating temperature range. [35,36] The common optical transparent SMPs, such as polyacrylate, poly(*tert*-butylacrylate), polyurethane, polycarbonate, and so on [37–39], possess a relatively lower deformation temperature, and it can hardly be applied for the devices operating at high temperature. Shape memory polyimide, as the unique SMP possesses a series of merits, except for the shape memory effect, it still provides a wide service temperature and excellent thermal oxidation stability, which can be used for the devices operating at extreme conditions. [40–43] In our previous works, it has been certified that the colorless shape memory polyimide exhibits broad prospects in advanced optoelectronics for excellent optical transparency, decent active deformation capacity and high temperature resistance [44–46].

In this study, the transformable flexible transparent graphene electrode was prepared by combining CVD-grown graphene and the transparent shape memory polyimide (TSMPI) films. The single-layer graphene film was grown on the Cu foil with a decent electrochemical polishing technology, and then graphene was transferred onto TSMPI films using the casting film property of TSMPI. The electrochemical polished Cu foil possesses a smooth surface with a Ra of 22 nm and Rq of 28 nm, which is quite fitting to the growth of the graphene with flawless structure. The single-layer graphene transferred from Cu substrates to the target TSMPI matrix by the facile direct-peeling method (Fig. 1a) only undergoes one interface transfer, which can avoid the irreversible damage of multiple transfer processes. The average sheet resistance of the graphene electrode is 310 Ω/sq, and the luminance efficiency of the prepared flexible OLED is up to 4.9 cd/A at the current density of 1.12 mA /cm^2. In addition, the TSMPI flexible electrode endows the OLED with a property of shape memory, the prepared cylindrical OLED could recover the original two-dimensional shape from a temporary three-dimensional shape without the external support at the trigger temperature of 240 °C, and the flexible electrode can keep the stabilized R-to-R$_o$ ratio during a 2000 cycles continuous bending process. It can be foreseeable that the pG@TSMPI opens a vast prospect of extensible visibly transparent solar cells.

2. Experimental section

2.1. Materials

2,2′-bis(trifluoromethyl)-4,4′-diaminobiphenyl (TFDB) (98%) and 4,4′-(4,4′-Isopropylidenediphenoxy) diphthalic Anhydride (BPADA) (98%) were purchased from Aladdin LLC. Chromatographically pure dimethylacetamide (DMAc) was purchased from Tianjin Guangfu Fine Chemicals Institute. All chemical reagents were used in the experiments directly without further treatment. The *ortho*-phosphoric acid was chosen as electropolishing solution [47].

2.2. Electrochemical polishing Cu foil

Firstly, the Cu foil was successively soaked in acetone, 1 M acetic acid solution and deionized water ultrasonic cleaning for 10 min to remove organic oil stains and oxidation layer on the surface of the Cu foil. The cleaned Cu foil and cathode copper sheet were fixed by a platinum electrode clamp and placed parallelly, and immersed in the electropolishing solution completely, the distance between the anode and cathode was controlled to be 4 cm. Under the constant voltage mode of the electrochemical workstation, 4 ~ 5 V working voltage was applied to control the polishing time of 60 ~ 180 s. After polishing, the Cu foil was taken out and rinsed it continuously with deionized water for 5 min each time for 3 times, finally soak it with anhydrous ethanol for 10 min, and drying it for later use.

2.3. Preparation and transfer of single-layer graphene

The pretreated Cu base is placed in the quartz boat and pushed into the heating area of the tube furnace. The vacuum degree of the chamber was pumped to 0.5 ~ 0.7 Pa, and hydrogen was pumped into the chamber. The hydrogen flow rate was set at 10 sccm. At the same time, The Cu foils were annealed at 1040 °C with a heating rate of 25 °C/min in hydrogen for 30 min. And then, reheat to 1040 °C with 10 sccm of hydrogen and 15 sccm of methane simultaneously injected for 30 min. The monolayer graphene film with Cu foil substrate was removed when it came down to room temperature with a cooling rate of 30–40 °C/min under the condition that the flow rate of hydrogen and methane remained unchanged and argon gas was injected into the chamber until the pressure of the tube dropped to atmospheric pressure.

The transparent shape memory polyimide (TSMPI) can refer to our previous work [44], and the tape-casting solution was the DMAc with 15 wt% TSMPI. Paving the Cu foil with graphene growing on, the Cu foil was fixed on a glass pane by the heat release tape (Semiconductor Equipment Corporation, 3195 V), and the TSMPI solution was dropped directly on the Cu foil surface to form a coating film. Drying in the oven for 80 °C/10 h and 120 °C/4h, the sandwich layer structure of Cu foil/monolayer graphene/TSMPI was obtained after the solvent was completely volatilized. Heating the glass pane to 170 °C, the heat release tape was separated from the copper foil. Finally, the copper foil substrate was etched with a ferric chloride etching solution. The TSMPI film with monolayer graphene was obtained by rinsing it twice with anhydrous ethanol and deionized water.

2.4. Fabrication of smart OLED

(I) Electrode pattern was carried out on the transferred pG@TSMPI by using high adhesive tape, and the pG@TSMPI was cleaned with deionized water and anhydrous ethanol, respectively and drying it;

(II) A 2 nm molybdenum trioxide layer was deposited on the surface of pG@TSMPI by vacuum evaporation with the chamber vacuum control lower than 5 × 10^{-4} Pa and the evaporation rate of 0.2–0.3 nm/s; the conductive polymer PEDOT: PSS solution was filtered by a water-based syringe filter with a diameter of 0.45 μm, and rotated it on the surface of the electrode by a rotary coating process.

(III) The electrode was annealed by a plate heating table in an air atmosphere with the annealing temperature at 120 °C for 20 min. By adjusting the rotation speed, the PEDOT:PSS thickness after annealing is about 30 nm.

(IV) The composite luminescent polymer solution with a concentration of 10 mg/ mL was prepared by dissolving MEH-PPV and PFO in toluene solvent and mixed together to obtain. The composite luminescent layer was rotated on the surface of PEDOT:PSS film and dried under nitrogen (80 °C, 30 min) and the thickness of the luminescent layer was controlled to be about 80 nm.

(V) The layer of Cs_2CO_3 film around 2 nm was coated on the surface of the luminescent layer by vacuum thermal evaporation. Then a layer of aluminum cathode metal of about 150 nm was and covered with a vacuum degree lower than 5 × 10^{-4} Pa and the evaporation rate was controlled to 1 ~ 2 nm/s.

3. Result and discussion

It is reported that typical electrochemical polishing technology is the common surface treatment method of metal items, allowing smooth and brightening of rough metal surfaces [48,49]. Herein, the Cu foil was handled with electrochemical polishing before the graphene layer is grown, and the electrochemical polishing device and mechanism are shown in Fig. 1b ~ c. With the energization of direct current, the rugged surface of Cu foil will form an uneven dense layer at the microscale. In contrast, the viscous layer of the hump part is thinner than others, which results in a lower resistance and contributes to the accumulation of

positive charge. Eventually, the rich-charged hump part will dissolve faster under a higher current density and polish the rough surface of Cu foil.

The craft of electrochemical polishing is crucial to the evenness of Cu foil, and the linear sweep voltammetry (LSV) characteristic curve was measured to confirm the optimum polishing parameters. It can be seen from Fig. 1d that the LSV curves show a steady current during the voltage of 4.0 V ~ 5.0 V, which means that the Cu foil surface formed a stable viscous layer. Therefore, 4.5 V was chosen as the polishing voltage, and Fig. 1e provides the variational current curve with time at a constant polishing voltage. After a rapid decline process, the current begins to stabilize at around 60 s, corresponds to the formation of a stable viscous layer on the surface of Cu foil.

To obtain an appropriate polishing surface, the effect of different polishing times to Cu foil was also researched. The optical microscope image and SEM image of the pristine Cu foil surface are shown in Fig. 2a and Fig. 2e, respectively, it can be seen that there are abundant parallel stair-like micro embossments arranged in the original unpolishing Cu foil surface, which are the manufactured trails of the Cu foil. In addition, AFM was carried out to characterize the microstructure of the surface in depth. The unpolishing Cu foil surface exhibits a dramatically altitude variation at the micron-level (Fig. 2i), and the arithmetic mean deviation (Ra) and root mean square deviation (Rq) of the surface roughness up to 143 nm and 190 nm, respectively. When graphene is grown on this kind of surface by CVD experiment, it will form the sundry defects of crystal boundary because of the bumpy embossment. The rougher of the surface, the larger the nucleus density of grown graphene, and the more defect of the obtained graphene will exist, which is unfavorable for the conductivity of obtained graphene. After a 60 s electrochemical polishing process, a relatively gentle surface was obtained (Fig. 2b and Fig. 2f), and the AFM image (Fig. 2j) shows that the Ra and Rq of surface roughness declined to 85 nm and 102 nm, respectively, which has been flat relatively. However, the residual striped embossment means 60 s is not a decent polishing time. When the electrochemical polishing time was employed to 180 s, Fig. 2c and Fig. 2g exhibit a smoother surface with the disappearance of stripes and bumps, and the residual defective spots can be attributed to the impurities during the manufacture of Cu foil. The AFM image (Fig. 2k) also presents a gentle variation of roughness with the appropriate Ra (22 nm) and Rq (28 nm), which are quite fitting for growing the graphene with a perfect lattice structure. A further polishing process was also studied. However, the long polishing time of 240 s brings the Cu foil to an inferior surface with plentiful potholed erosion (Fig. 2d, Fig. 2h, and Fig. 2l), which can be ascribed to the break of stable viscous layer causing the formed new anode to dissolve and generate amounts of oxygen at the surface, and the attached oxygen bubble evolve into the potholed erosion surface eventually. Hence, 180 s is a decent handle time for electrochemical polishing Cu foil to obtain a smooth surface for graphene growth.

For this study, the CVD conditions, similar to those reported in previous reports were used for growing the graphene on the Cu foil treated by electrochemical polishing, and more details are described in the experimental section. After the CVD procession, a direct-peeling method was used to transfer graphene on TSMPI film with the unique coating film property of TSMPI. As shown in Fig. 1a, a heat release tape fixed roping the Cu foil grown with graphene on a glass pane, and the polyimide solution dropped directly on the Cu foil surface to form a coating film. After drying the solvent, the TSMPI film-attached monolayer graphene was obtained with the tape released by heating and Cu foil removed by etching. This is an excellent transferred method of graphene grown through CVD as the following merits: firstly, the target substance works as a supporting matrix directly, which will avoid the extra pollution towards transferred graphene and obtain the graphene

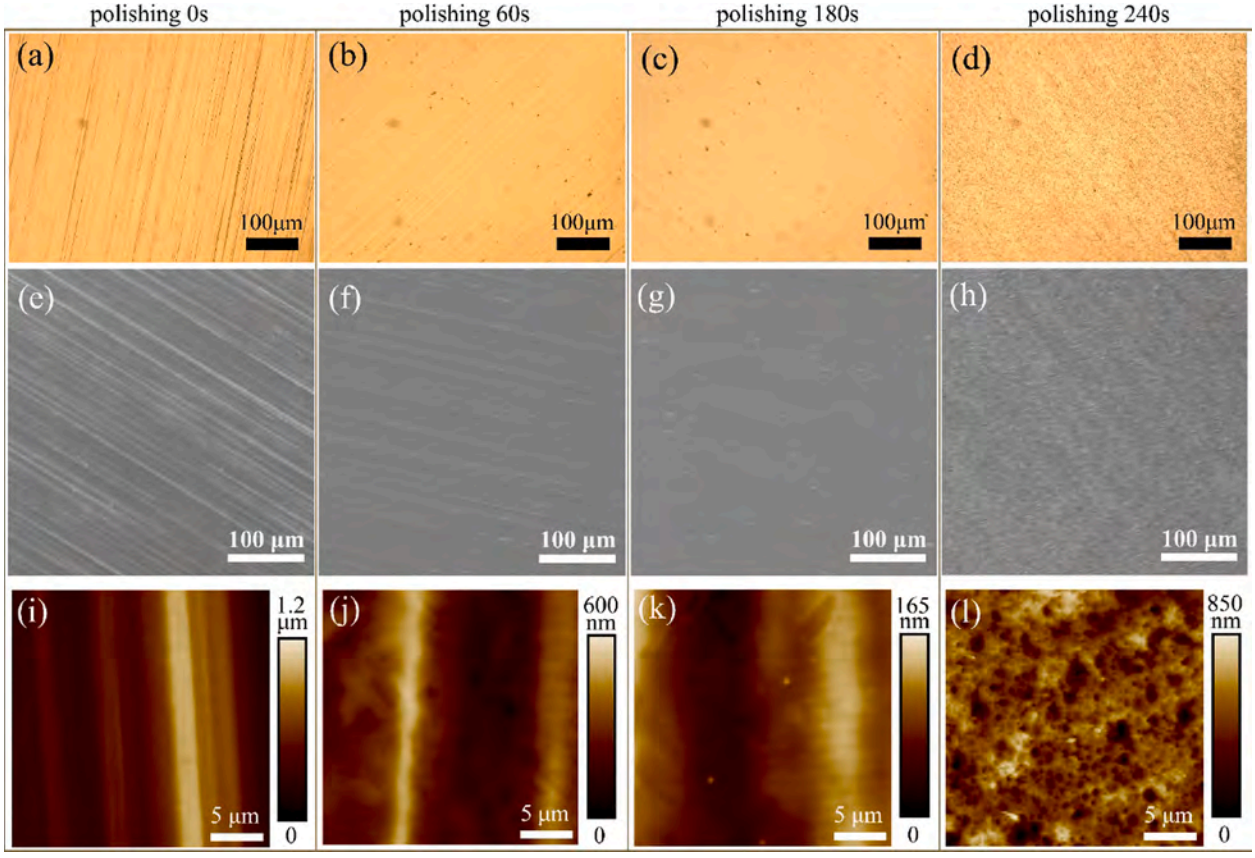

Fig. 2. Optical microscope image of copper foil with polishing time of a) 0 s; b) 60 s; c) 180 s; d) 240 s; SEM image of copper foil with polishing time of e) 0 s; f) 60 s; g) 180 s; h) 240 s; AFM image of copper foil with polishing time of i) 0 s; j) 60 s; k) 180 s; l) 240 s.

with an ultra-clean surface; secondly, the convenient and flexible operation process will enhance the stability and repeatability of the transferred process because of the reducing of redundant manual operation; the more critically, the transferred procession can hardly bring flaws to graphene, which protects the continuity and integrity of grown graphene and enable the superior electroconductibility to the graphene electrode.

Raman spectra are a powerful tool for identifying the lattice structures, and it was used to characterize the lattice species of grown graphene. The Raman spectra of the graphene grown on Cu foil were tested directly, and Fig. 3a illustrates the analysis result removing the background of Cu foil. Two main peaks appeared at 1580 cm^{-1} and 2700 $cm^{-1,}$ in the graphene grown on the polished and unpolished Cu foil, which belong to the G band and 2D band, respectively. The D band, around 1350 cm^{-1} presents the defect and disorder of carbon atom, was not detected, which means that the obtained graphene film both are highly regular with rare structure defects. In addition, both the 2D peaks belong to the symmetric and unitary Lorentz peak, and the intensity ratio of 2D-to-G was more significant than 1, which means that it is a monolayer of the graphene layer grown on the Cu foil. The two-dimension Raman image was scanned with the I_{2D}/I_G ratio as pixels unit. The I_{2D}/I_G mean value of the graphene grown on the unpolished Cu foil (uG@Cu) is around 1.5 (Fig. 3b), while the value of the graphene grown on the polished Cu foil (pG@Cu) up to 2.3 (Fig. 3c). The I_{2D}/I_G distribution of pG@Cu is more homogeneous than uG@Cu, which illustrates that the pG@Cu possesses a high quality for the less defects, and it can be attributed to the gentle surface of polished Cu foil endows a minority nucleus density of graphene with slight lattice defects.

Microscopic studies were also carried out to observe the surface morphology of the graphene films before and after the transfer of TSMPI. Fig. 4a exhibits a Laser scanning confocal microscope (LSCM) of the uG@Cu, and it can be seen that the initial parallel stair-like micro embossment of Cu foil was vanished after high temperature annealing of the CVD process and replaced by reconstructed polymorphism morphology. The interior of crystalline grains were relatively flat, but there are still some cupped crystal boundary between grains in the copper surface arranged randomly, where the graphene will nucleate primarily at these grains boundaries and bring a more significant nucleus density of whole graphene, which will form more defects of polycrystalline and be harmful to the structural integrity of graphene films. After the transfer via TSMPI, the LSCM image (Fig. 4b) shows that the transferred graphene duplicated the polycrystalline structure completely, and the convex steps morphology on the surface corresponded to the cupped morphology of the grain boundary. The transferred result also demonstrates that the etching of Cu foil will not destroy the continuity and integrity of the graphene layer as the remaining convex steps morphology after stripping reversely, which can be attributed to the in-depth infiltration of PI solution at crystal boundaries. AFM was conducted to characterize the microstructure after transfer further. Fig. 4c shows that the height variation of uG@TSMPI up to micron level, the steps morphology at grain boundaries bring the Ra near to 96 nm, and this microstructure with convex steps will against the preparation of OLED because of the raised graphene is easy to puncture the luminous layer and further cause the short circuit. Fig. 4d and Fig. 4e present the LSCM images of pG@Cu before and after the transfer via TSMPI. Fig. 4d shows a gentle morphology of pG@Cu, and compared with uG@Cu, the pG@Cu possesses a smaller nucleus density with a large crystallite dimension and a shallow grain boundary after high temperature annealing of the CVD process, which endows a high quality to graphene layer with fewer lattice defects. The microscopic morphology result is consistent with the analysis of Raman spectra. After the transfer of TSMPI, the duplicated structure displays a gently undulating microscopic morphology with a mild variation of the horizon (Fig. 4e), and it can be regarded as a smooth surface to some extent. The

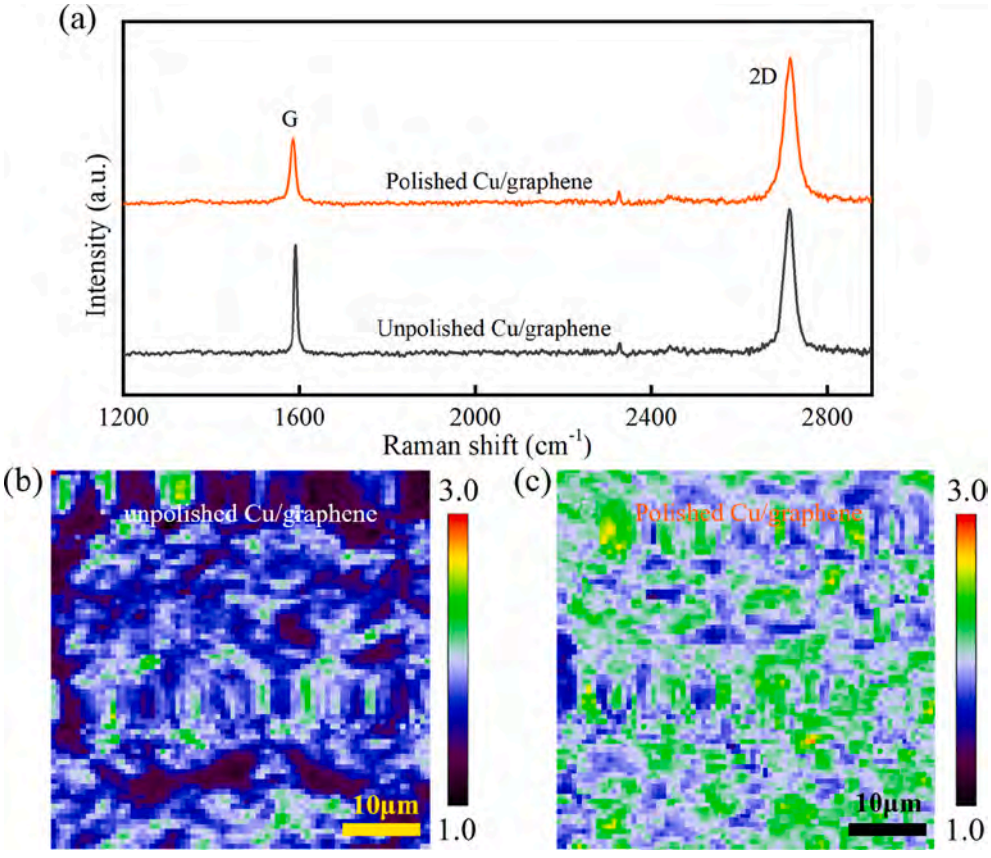

Fig. 3. a) Raman spectra of monolayer graphene; The I_{2D}/I_G Raman mapping image of graphene on b) unpolished copper-foil; c) polished copper-foil.

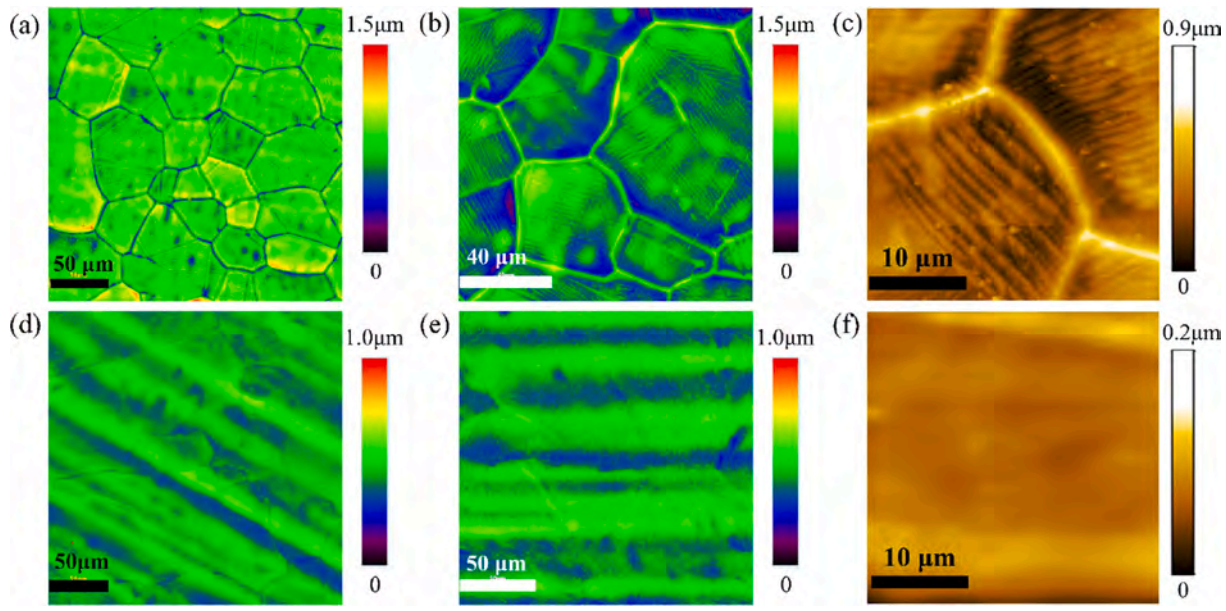

Fig. 4. LCM image of a) graphene on unpolished copper foil; b) transferred graphene on unpolished copper foil; c) graphene on polished copper foil; d) transferred graphene on polished copper foil; AFM image of e) transferred graphene on unpolished copper foil; f) transferred graphene on polished copper foil.

AFM image of pG@TSMPI (Fig. 4f) exhibits a gentle surface microstructure, showing only nano-level variation of height. The Ra is 18 nm, suggesting a quite flat surface. Without the participation of the as other supporting layers during the transfer process, the obtained graphene layer was undefiled without any pollution and impurity, which lays a solid foundation for the graphene electrode and high-performance OLEDs.

The structure and properties of TSMPI had been well studied in our previous works [44]. The FTIR spectra of flow-casted TSMPI film were given in Fig. 5a, and the characteristic peaks of TSMPI were correspond to the structure as the previous report. The absorption peaks at around 1781 cm^{-1} and 1720 cm^{-1} belong to the vibration of C = O, and the absorption peak at 1357 cm^{-1} is the vibration of the C–N–C bond, demonstrate demonstrating the structure of SMPI.

The transparency of TSMPI based monolayer graphene was examined by Ultraviolet–visible spectroscopy (UV–Vis), and Fig. 5b shows the transmittance of different films at the wavelength from 400 nm to 800 nm (the inset picture is the digital photo of pG@TSMPI). The pure TSMPT film shows a transmittance of 90% at 550 nm, while the transparency of uG@TSMPI and pG@TSMPI is down to 84.6% and 85.5%, respectively, due to the absorption of visible light by the graphene layer. The distinction of the twain transmittance is not obvious, and both meet the requirements of transparent electrodes for optoelectronic devices such as OLED and OPV. It is reported that the theoretical absorption of monolayer graphene at 550 nm is about 2.3% [7]. In contrast, the actual absorption of obtained graphene exceeded the value mildly, which can account for the graphene layer after the transfer was not flat strictly for the undulating character of Cu foil morphology, and combined with the multi-layer fold of graphene at grain boundary, these enhanced the scattering of graphene layer towards visible light jointly and lead to a lower practical transmittance. Although the transparency of prepared electrodes is less than 90%, they still can be regarded as decent transparent electrodes compared with the analogous electrodes.[7].

Four point probe was used to test the square resistance of flexible graphene film, the uG@TSMPI and pG@TSMPI present a uniform resistance distribution with the average resistance value of 420 ± 22 Ω and 310 ± 18, respectively. The pG@TSMPI exhibits a more excellent electrical conductivity for less lattice defects, which demonstrates the superiority of electrochemical polishing technology. Further, the property of flexural fatigue was also conducted to evaluate the conductive stability of flexible transparent electrodes. The inset picture of Fig. 5c gives the bending cycle process of pG@TSMPI, and the resistance ratio before (R_o) and after (R) bending behind each 100 cycles of continuous operation was used to describe the flexural fatigue of flexible electrodes. As can be seen from Fig. 5c, during a 2000 cyclic bending process, the R-to-R_o ratio stabilized at around 1.02 from beginning to end, which illustrates the excellent mechanical flexibility and fatigue resistance of pG@TSMPI. The thickness of ultrathin monolayer graphene is only 0.34 nm, which possesses the beautiful property of deformed adaptation, and enables the tight contact between the transferred graphene and the TSMPI matrix during the bending process.

To confirm the practicability of the flexible transparent electrode, a graphene-based white OLED with the pG@TSMPI/MoO_3/poly (3,4-ethylenedioxythiophene) polystyrene sulfonate (PEDOT:PSS)/0.5 wt% MEH-PPV/Cs_2CO_3/Al structure was fabricated, and Fig. 5d illustrates the device structure specifically. Subsequently, the optical and electrical properties of the flexible transparent OLED device were investigated. Fig. 5e describes the current density–voltage characteristics of the OLED, and the device presents the rectification effect. During the low voltage range, it shows that the current density rises slowly with the voltage increase. When the voltage applied exceeds a critical value, the current density grown exponentially as the voltage increases. With the further increase of voltage, the slows break down current density rise slows until the device breaks down at the maximal current density of 280 mA/cm^2. Fig. 5e also shows the luminance-voltage curve of OLED, it can be seen that the luminance rises slowly with the increase of voltage at the primary stage, while once over the activation voltage at 5.8 V, the luminance rises rapidly with the increase of voltage, and the maximal luminance up to 4970 cd/cm^2. The luminance efficiency-current density characteristics of OLED are given in Fig. 5f. The luminance efficiency increased as the current density increased until the efficiency up to the peak value of 4.9 cd/A with the current density of 1.12 mA $/cm^2$, which was similar to the performance of the ITO electrode device with the same structure. The excellent optical and electrical properties of prepared OLEDs show the flexible transparent electrode a bright prospect in photoelectric devices.

As a kind of shape memory material, the flexible and transparent matrix TSMPI endows the OLED device with a reversible shape reconstruction property with spontaneous deformation and variable stiffness, which can deform the device from a simple two-dimensions structure to

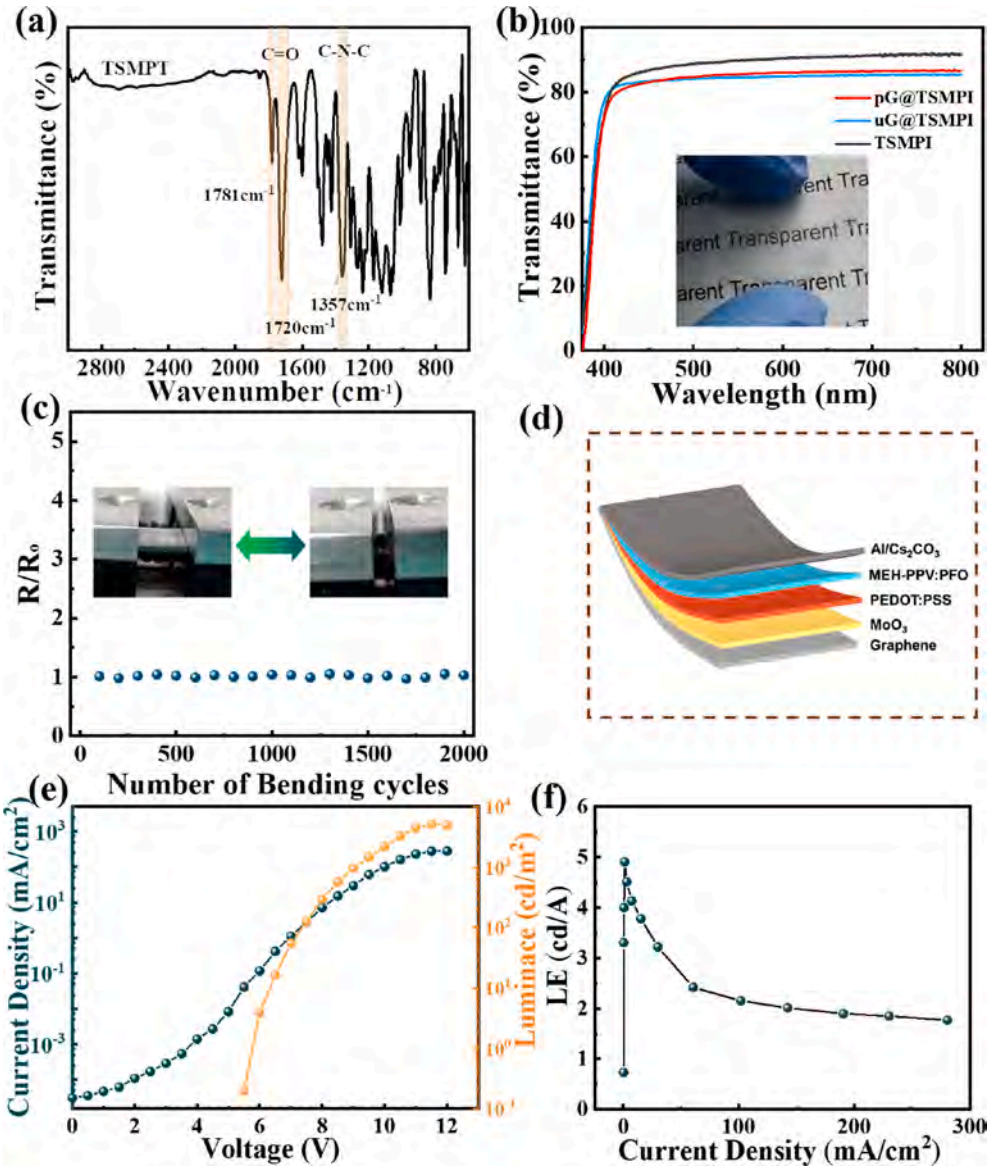

Fig. 5. a) ftir spectra of tsmpi; b) UV–Vis absorption spectra of flexible monolayer graphene; c) Resistance of pG@TSMPI variation over bending cycles, the inset picture shows the bending process; d) Device structure diagram of graphene-based white OLED; e) Current density–voltage characteristic curve and Luminance-voltage characteristic curve; f) Luminance efficiency-current density characteristic curve.

a complex three-dimensions structure and maintain the temporary shape stably without the supporting of external force. Figure 6a shows the shape recovery process of pG@TSMPI-based OLED from a cylinder three-dimensions shape recovery to planar two-dimension shape. The cylinder OLED was deformed to the primary shape in 15 s triggered at the temperature of 240 °C, which presents the device with a good shape memory performance. To identify the luminescence property of the pG@TSMPI-based OLED, Figure 6b shows that the device with a plane shape was illuminated at 9 V, and the light-emitting area is about 12 mm^2. When the device was heated to 240 °C, the TSMPI matrix endows the OLED property to deform into another shape, and the given shape could be fixed with the colling of temperature. The deformed shape can maintain the structure chronically without any external force or supporting power until reheating the devices are to the deformation temperature. Figure 6c shows that the OLED with a fixed cylindric shape can still be illuminated at 9 V, which presents the luminous stability of the pG@TSMPI electrode. Compared with the traditional transparency electrode, the pG@TSMPI electrode, which is equipped with excellent shape memory performance and luminescence properties could be applied to flexible electronic devices with the demand for shape reconstruction and voluntary deformation, such as space solar batteries, touch screen and the luminescent devices with complex shape.

4. Conclusion

The structural flawless graphene was grown on the electrochemically polished Cu foil by CVD, and transferred by the TSMPI to prepare the flexible transparent graphene electrodes. Without the participation of the supporting layer during the transfer process, the obtained flexible graphene electrode pG@TSMPI was ultra-clean and smooth. The transparent electrode possesses a light transmittance of 86% at 550 nm, an average sheet resistance of 310 Ω/sq, and a surface roughness Ra of 18 nm, which shows excellent optical and electrical properties. Except for the excellent luminescence performance, which can be comparable to that of ITO-based device, the pG@TSMPI-based smart white OLED possess the property of variable stiffness and reconfigurable shape because of the decent shape memory performance of TSMPI substrate, which brings the OLED a capacity transform from the 2D structure into a

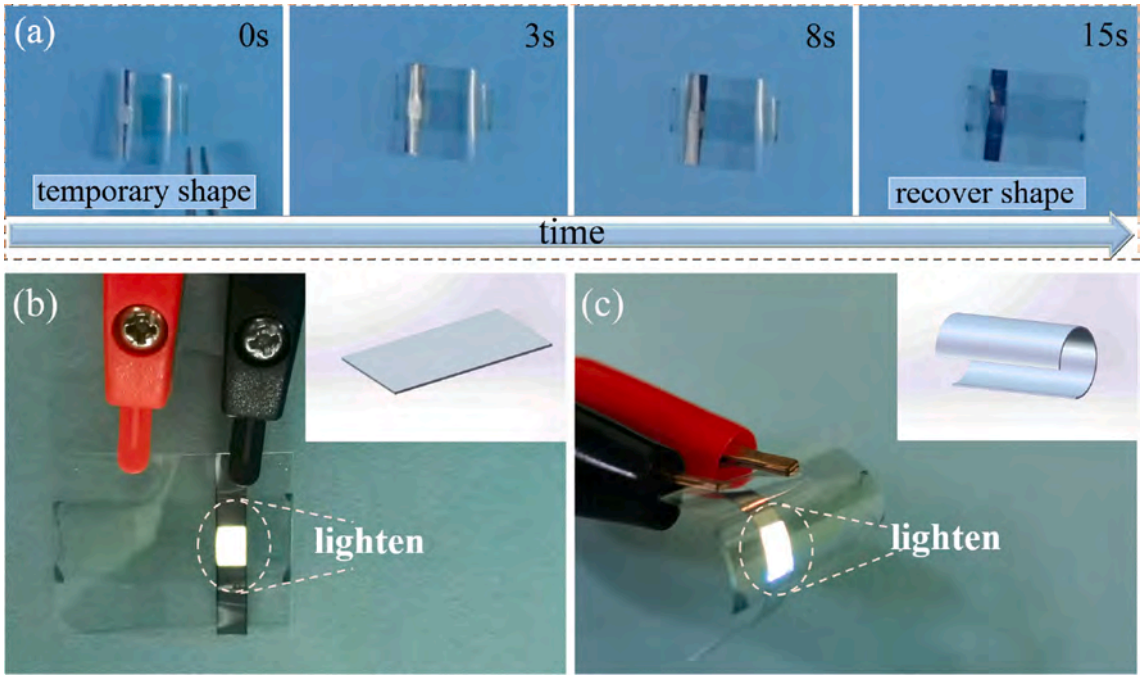

Fig. 6. a) shape memory recovery process of the 3D cylindrical OLED; lighted pG@TSMPI-based OLED at 9 V with b) planar two-dimension shape and c) cylinder three-dimensions shape.

complex 3D structure with the time going under deformation trigger temperature. This study opens up a new possibility for flexible transparent graphene electrode application, The combination of graphene and transparent SMP will obtain a high-quality SMP-based graphene electrode, and it can contribute to realizing the smart OLED devices with the capacity of deforming reversibly.

CRediT authorship contribution statement

Xinzuo Huang: Methodology, Investigation, Data curation. **Rongxiang Hu:** Writing – original draft. **Fenghua Zhang:** Writing – review & editing, Project administration. **Yanju Liu:** Resources, Supervision. **Jinsong Leng:** Resources, Supervision, Funding acquisition.

Declaration of Competing Interest

The authors declare that they have no known competing financial interests or personal relationships that could have appeared to influence the work reported in this paper.

Data availability

The data that has been used is confidential.

Acknowledgements

This work was financially supported by the National Key R&D Program of China (2022YFB3805700).

References

[1] Ellmer K. Past achievements and future challenges in the development of optically transparent electrodes. Nat Photonics 2012;6(12):808–16.
[2] Li Y, Xu G, Cui C, Li Y. Flexible and Semitransparent Organic Solar Cells. Adv Energy Mater 2018;8(7).
[3] Lee HB, Jin W-Y, Ovhal MM, Kumar N, Kang J-W. Flexible transparent conducting electrodes based on metal meshes for organic optoelectronic device applications: a review. J Mater Chem C 2019;7(5):1087–110.
[4] Hofmann AI, Cloutet E, Hadziioannou G. Materials for Transparent Electrodes: From Metal Oxides to Organic Alternatives. Adv Electron Mater 2018;4(10).
[5] Raman V, Cho Y-H, Park J-H, Chinnadurai D, Kim H-K. Impact of low temperature plasma annealing for flexible, transparent and conductive ITO/PEDOT:PSS composite electrode. J Ind Eng Chem 2021;93:423–9.
[6] Mustonen P, Mackenzie DMA, Lipsanen H. Review of fabrication methods of large-area transparent graphene electrodes for industry. Front Optoelectron 2020;13(2):91–113.
[7] Song Y, Zou W, Lu Q, Lin L, Liu Z. Graphene Transfer: Paving the Road for Applications of Chemical Vapor Deposition Graphene. Small 2021;17(48):e2007600.
[8] Forrest SR. The path to ubiquitous and low-cost organic electronic appliances on plastic. Nature 2004;428(6986):911–8.
[9] Leterrier Y, Medico L, Demarco F, Manson JAE, Betz U, Escola MF, et al. Mechanical integrity of transparent conductive oxide films for flexible polymer-based displays. Thin Solid Films 2004;460(1–2):156–66.
[10] Chen J-H, Jang C, Xiao S, Ishigami M, Fuhrer MS. Intrinsic and extrinsic performance limits of graphene devices on SiO2. Nat Nanotechnol 2008;3(4):206–9.
[11] Son DR, Raghu AV, Reddy KR, Jeong HM. Compatibility of Thermally Reduced Graphene with Polyesters. Journal of Macromolecular Science, Part B 2016;55(11):1099–110.
[12] Babu A, Somesh TE, Ani Dechamma CD, Hemavathi AB, Kakarla RR, Kulkarni RV, et al. Ternary structured magnesium cobalt oxide/graphene/polycarbazole nanohybrids for high performance electrochemical supercapacitors. Materials Science for Energy Technologies 2023;6:399–408.
[13] M.A.S. Badri, M.M. Salleh, N.F.a.M. Noor, M.Y. Abd Rahman, A.A. Umar, Green synthesis of few-layered graphene from aqueous processed graphite exfoliation for graphene thin film preparation, Materials Chemistry and Physics 193 (2017) 212-219.
[14] Regis J, Vargas S, Irigoyen A, Bramasco-Rivera E, Banuelos JL, Delfin LC, et al. Near-UV light assisted green reduction of graphene oxide films through l-ascorbic acid. International Journal of Smart and Nano Materials 2021;12(1):20–35.
[15] Wu M, Chen J, Wen Y, Chen H, Li Y, Li C, et al. Chemical Approach to Ultrastiff. Strong, and Environmentally Stable Graphene Films, Acs Applied Materials & Interfaces 2018;10(6):5812–8.
[16] Zhang F, Yang K, Liu G, Chen Y, Wang M, Li S, et al. Recent advances on graphene: Synthesis, properties and applications. Compos A Appl Sci Manuf 2022;160.
[17] Huang X, Zeng Z, Fan Z, Liu J, Zhang H. Graphene-Based Electrodes. Adv Mater 2012;24(45):5979–6004.
[18] Xu Y, Liu J. Graphene as Transparent Electrodes: Fabrication and New Emerging Applications. Small 2016;12(11):1400–19.
[19] Bae S, Kim H, Lee Y, Xu X, Park J-S, Zheng Y, et al. Roll-to-roll production of 30-inch graphene films for transparent electrodes. Nat Nanotechnol 2010;5(8):574–8.
[20] Morin JLP, Dubey N, Decroix FED, Luong-Van EK, Castro Neto AH, Rosa V. Graphene transfer to 3-dimensional surfaces: a vacuum-assisted dry transfer method, 2d. Materials 2017;4(2).
[21] Hong N, Kireev D, Zhao Q, Chen D, Akinwande D, Li W. Roll-to-Roll Dry Transfer of Large-Scale Graphene. Adv Mater 2022;34(3):e2106615.
[22] Zhang D, Zhang Q, Liang X, Pang X, Zhao Y. Defects Produced during Wet Transfer Affect the Electrical Properties of Graphene. Micromachines (Basel) 2022;13(2).

[23] Zhang Z, Xia L, Liu L, Chen Y, Wang Z, Wang W, et al. Ultra-smooth and robust graphene-based hybrid anode for high-performance flexible organic light-emitting diodes. J Mater Chem C 2021;9(6):2106–14.
[24] Ullah S, Yang X, Ta HQ, Hasan M, Bachmatiuk A, Tokarska K, et al. Graphene transfer methods: A review. Nano Res 2021;14(11):3756–72.
[25] Ali S, Ahmad F, Yusoff PSMM, Muhamad N, Oñate E, Raza MR, et al. A review of graphene reinforced Cu matrix composites for thermal management of smart electronics. Compos A Appl Sci Manuf 2021;144.
[26] Bai S, Guo X, Chen T, Zhang Y, Zhang X, Yang H, et al. Solution processed fabrication of silver nanowire-MXene@PEDOT: PSS flexible transparent electrodes for flexible organic light-emitting diodes. Compos A Appl Sci Manuf 2020;139.
[27] Xia Y, He Y, Zhang F, Liu Y, Leng J. A Review of Shape Memory Polymers and Composites: Mechanisms, Materials, and Applications. Adv Mater 2021;33(6).
[28] Fulati A, Uto K, Iwanaga M, Watanabe M, Ebara M. Smart Shape-Memory Polymeric String for the Contraction of Blood Vessels in Fetal Surgery of Sacrococcygeal Teratoma. Advanced Healthcare Materials; 2022.
[29] Zhang F, Wen N, Wang L, Bai Y, Leng J. Design of 4D printed shape-changing tracheal stent and remote controlling actuation. International Journal of Smart and Nano Materials 2021;12(4):375–89.
[30] Herath M, Emmanuel C, Jeewantha J, Epaarachchi J, Leng J. Distributed sensing based real-time process monitoring of shape memory polymer components. J Appl Polym Sci 2022;139(22).
[31] Yang S, He Y, Leng J. Shape memory poly (ether ether ketone)s with tunable chain stiffness, mechanical strength and high transition temperatures. International Journal of Smart and Nano Materials 2022;13(1):1–16.
[32] Gaj MP, Wei A, Fuentes-Hernandez C, Zhang Y, Reit R, Voit W, et al. Organic light-emitting diodes on shape memory polymer substrates for wearable electronics. Org Electron 2015;25:151–5.
[33] Yu Z, Zhang Q, Li L, Chen Q, Niu X, Liu J, et al. Highly Flexible Silver Nanowire Electrodes for Shape-Memory Polymer Light-Emitting Diodes. Adv Mater 2011;23(5):664-+.
[34] Yu Z, Niu X, Liu Z, Pei Q. Intrinsically Stretchable Polymer Light-Emitting Devices Using Carbon Nanotube-Polymer Composite Electrodes. Adv Mater 2011;23(34):3989-+.
[35] Lei M, Xu B, Pei Y, Lu H, Fu YQ. Micro-mechanics of nanostructured carbon/shape memory polymer hybrid thin film. Soft Matter 2016;12(1):106–14.
[36] Qian C, Wang D, Zhao W, Yang W, Qin Z, Zhu Y, et al. Smart shape memory composite foam enabled rapid and conformal manipulation of electromagnetic wave absorption performance. Materials Today Nano 2023;23.
[37] Yu Z, Zhang Q, Li L, Chen Q, Niu X, Liu J, et al. Highly flexible silver nanowire electrodes for shape-memory polymer light-emitting diodes. Adv Mater 2011;23(5):664–8.
[38] Jung YC, Kim HH, Kim YA, Kim JH, Cho JW, Endo M, et al. Optically Active Multi-Walled Carbon Nanotubes for Transparent. Conductive Memory-Shape Polyurethane Film, Macromolecules 2010;43(14):6106–12.
[39] Xiao X, Qiu X, Kong D, Zhang W, Liu Y, Leng J. Optically transparent high temperature shape memory polymers. Soft Matter 2016;12(11):2894–900.
[40] Lim H, Cho WJ, Ha CS, Ando S, Kim YK, Park CH, et al. Flexible organic electroluminescent devices based on fluorine-containing colorless polyimide substrates. Adv Mater 2002;14(18):1275-+.
[41] Lim J-W, Cho D-Y, Eun K, Choa S-H, Na S-I, Kim J, et al. Mechanical integrity of flexible Ag nanowire network electrodes coated on colorless PI substrates for flexible organic solar cells. Sol Energy Mater Sol Cells 2012;105:69–76.
[42] Sidler K, Cvetkovic NV, Savu V, Tsamados D, Ionescu AM, Brugger J. Organic Thin Film Transistors on Flexible Polyimide Substrates Fabricated by Full Wafer Stencil Lithography. In: 23rd Eurosensors Conference; 2009. pp. 762-+.
[43] Wang X, He Y, Leng J. Shape memory polyimides and composites with tunable chain stiffness and ultrahigh transition temperature range. Compos A Appl Sci Manuf 2022;163.
[44] Huang X, Zhang F, Liu Y, Leng J. Flexible and colorless shape memory polyimide films with high visible light transmittance and high transition temperature. Smart Mater Struct 2019;28(5).
[45] Huang X, Zhang F, Leng J. Metal mesh embedded in colorless shape memory polyimide for flexible transparent electric-heater and actuators. Appl Mater Today 2020;21.
[46] Huang X, Zhang F, Liu Y, Leng J. Active and Deformable Organic Electronic Devices based on Conductive Shape Memory Polyimide. ACS Appl Mater Interfaces 2020;12(20):23236–43.
[47] Zhang B, Lee WH, Piner R, Kholmanov I, Wu Y, Li H, et al. Low-Temperature Chemical Vapor Deposition Growth of Graphene from Toluene on Electropolished Copper Foils. ACS Nano 2012;6(3):2471–6.
[48] Yao W, Zhang J, Ji J, Yang H, Zhou B, Chen X, et al. Bottom-Up-Etching-Mediated Synthesis of Large-Scale Pure Monolayer Graphene on Cyclic-Polishing-Annealed Cu(111). Adv Mater 2022;34(8):2108608.
[49] Nalini S, Thomas S, Jayaraj MK, Sudarsanakumar C, Kumar KR. Chemical vapour deposited graphene: substrate pre-treatment, growth and demonstration as a simple graphene-based SERS substrate. Bull Mater Sci 2020;43(1).